CrystEngComm

Accepted Manuscript

ROYAL SOCIETY OF CHEMISTRY

www.rsc.org/crystengcomm

Cite this: DOI: 10.1039/c3xx00000x

www.rsc.org/xxxxxx

PAPER

The Ce doping influence on the magnetic phase transition in In_2S_3:Ce nanoparticles

Binbin Yao[ab], Pan Wang [a], Shuangming Wang [a], Mingzhe Zhang*[a]

Received (in XXX, XXX) Xth XXXXXXXXX 20XX, Accepted Xth XXXXXXXXX 20XX

DOI: 10.1039/b000000x

The classical thermally driven from supermagnetic to blocked supermagnetic and the quantum phase transition from magnetic long-range order to quantum superparamagnetic state have been observed in ultrasmall In_2S_3:Ce diluted magnetic semiconductors (DMSs). The In_2S_3:Ce nanoparticles (5-6nm) have been synthesized by a facile gas-liquid phase chemical deposition process using $Ce(COOCH_3)_3$, $In(COOCH_3)_3$ and H_2S as source materials. X-ray diffraction (XRD), X-ray photoelectron spectroscopy (XPS) and high resolution transmission electron microscopy (HRTEM) have been used to characterize the structure, component, morphology and size. The photoluminescence emission spectrum (PL) demonstrates that the luminescence quantum efficiency increases as Ce addition and indicates the existence of Ce atoms in the structure. The magnetic property reflects a strong f-f exchange interaction between Ce ions. The Ce doped In_2S_3 nanoparticles are shown to exhibit the higher blocking temperature from superparamagnetic to magnetic long-range order state, and even to be room-temperature ferromagnetism. The larger ionic radius of Ce results in the larger influence on carrier concentration, and affecting the blocking temperature of magnetic phase transition.

Introduction

The nanoscale diluted magnetic semiconductors (DMSs) have been attracted increasing attention due to remarkable quantum size effect and the three-dimensional quantum confinement of electrons and holes.[1,2] Magnetic nanoparticles below Bohr excition radius exhibit superparamagnetic (SP), even quantum superparamagnetic (QSP). [3,4] The QSP provides the possibility for the mesoscopic magnets storge.[5] The nano DMSs combining diluted magnetic semiconductors and semiconductor quantum dots (QDs) have significant quantum size effect and the quantum confinement effect of electrons and holes.[6] It is possible to tune photoelectricity and magnetism as the particle size is decreased, also influence magnetic phase transition phenomenon.[7]

At present, minority experiment groups are pursing the synthesis of ultrasmall DMSs, and acquiring some achievements.[8,9] The results prove that ultrasmall DMSs exsit a complex magnetic behavior, such as, the magnetic phase transition from the SP driving from the thermal fluctuation of the random spin orientation to the SP be blocked; and the quantum phase transition from magnetic long-range order to QSP state.[9] People have done further research on the magnetic phase transition mechanism, but there is being challenge about the influencing factors of phase transition temperature.[9] Many studies suggest that the doped ions concentration influence the intensity of magnetization.[10] A nonhomogeneous distribution of doped atoms favors the formation of doped ions enriched areas and some isolated doped ions, resulting in the anti-ferromagnetism and paramagnetism.[11] It is visible that doping ions have important effects on magnetism. In addition, Hwang et al. show that the magnetic phase transition temperature decreases as the reduction of radius of doped ions.[12] If the ionic radius of doped ions is larger, resulting in the larger influence of carrier concentration, and effecting the magnetic phase transition.

In_2S_3 is a spinel structure with a larger amount of vacancies, showing the excellent physical properties.[13,14] In_2S_3 can act as a main material for the most metal ions due to the vacancies, not like other material that has the tendency to expel the object ions. In recent years, the studies of In_2S_3 are reported, focusing on the research of preparation methods and properties; [15,16] the optical property of doped In_2S_3 has been researched, [17,18] while there is few report about magnetism.[7] In this paper, we prepare ultrasmall In_2S_3:Ce nanoparticles with two magnetic phase transition and explore the magnetic mechanism, and further research the influence of Ce doping on magnetic phase transition.

Experimental

Ce^{3+} doped In_2S_3 nanoparticles were synthesized by gas-liquid phase chemical deposition. The experimental set-up and steps are shown in Fig.1. There were two reactive steps in the experiment. In the preparation step, the reactive solution was the mixture of $Ce(COOCH_3)_3$ (purity 99.99%), $In(COOCH_3)_3$ (purity 99.99%) and $HOCH_2CH_2SH$ in water according to the calculated amount. Then the pH value of the reaction solution was adjusted to 3.8～4.0 using CH_3COOH. The H_2S gas was prepared by HCl reacting with Na_2S according to the ratio of 1:1. In the reaction process, H_2S gas and the reactive solution reacted in a chamber with circulating water (25°C), which kept the stability of reaction

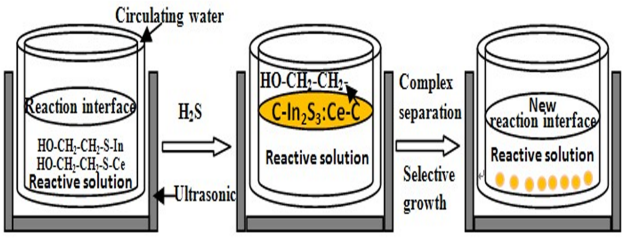

Fig.1 The scheme of the experimental set-up and steps.

conditions. The chamber was sited in the ultrasonic to avoid the nanoparticles forming aggregates and propel the new liquid surface emerging, and then which reacted with the flowing H_2S gas. In the beginning, numerous nuclei were formed and started to grow on gas-liquid interface. Under the effect of ultrasound, the particle invaded into the solution, the new liquid surface emerged. This process was repeated until reaction was fully completed. The precipitates were collected and washed with deionized water and anhydrous alcohol three times respectively, and dried in a nitrogen atmosphere.

The phase purity, structure and crystal size of the obtained products were observed with an X-ray diffraction (XRD) (Shimadzu, XRD-6000) and further analyzed with a high resolution transmission electron microscopy (HRTEM) (TECNAI G2) and an X-ray photoelectron spectroscopy (XPS) (ESCALAB MK II) .The photoluminescence (PL) spectroscopy was performed via a Perkin Elmer photoluminescence. The magnetic property was carried out by Quantum Design MPMS SQUID.

Results and Discussions

The phase purity and structure were determined by X-ray diffraction (XRD). Fig. 2(a) shows the XRD pattern of the In_2S_3:Ce nanoparticles with dopant content 0.71% and 0.91%. The broad peak at lower angle is fitted by two peaks (the green and blue one). The diffraction peaks are assigned to be tetragonal In_2S_3 phase according to JCPDS Cards (JCPDS card No. 25–390). Besides the tetragonal In_2S_3 phase, no others X-ray diffraction patterns associated with metallic Ce, CeS or Ce_2O_3 are observed showing that the nanoparticles are composed of pure phase. The peak position of the In_2S_3:Ce nanoparticles shifts slightly toward lower angle (higher d value) with increasing Ce content, suggesting an increase of lattice parameter. Doped Ce^{3+} can lead to lattice dilatation because the radius Ce^{3+} is bigger than In^{3+} radius. The Fig. 2(b) presents the Ce 3d X-ray Photoelectron Spectroscopy (XPS) spectrum of the In_2S_3:Ce nanoparticles. According to the result, the Ce $3d_{5/2}$ binding energy is 886.4 eV, and the Ce $3d_{3/2}$ binding energy is 902.1 eV. It shows that the Ce is in the Ce^{3+} state according to previous studies, [19,20] which excludes the possibility that magnetic behavior comes from the Ce metal clusters. From the XRD results, we do not see any Ce compounds either. Thus, it is strongly believed that we have successfully incorporated the rare-earth metal Ce^{3+} ions and dispersed them atomically in the In_2S_3 main structure.

The detailed micstructures of the prepared samples are characterized using High Resolution Transmission Electron Microscopy (HRTEM). In Fig. 3(a), we can see the diffraction rings corresponding to the X-ray diffraction pattern without any impurities, revealing only a single phase in the In_2S_3:Ce nanoparticles. The low resolution image displays the morphology of the prepared samples are particles with minisize. The lattice fringes of particles can be clearly seen, and the particles sizes are 5-6 nm as shown in Fig. 3 (b).

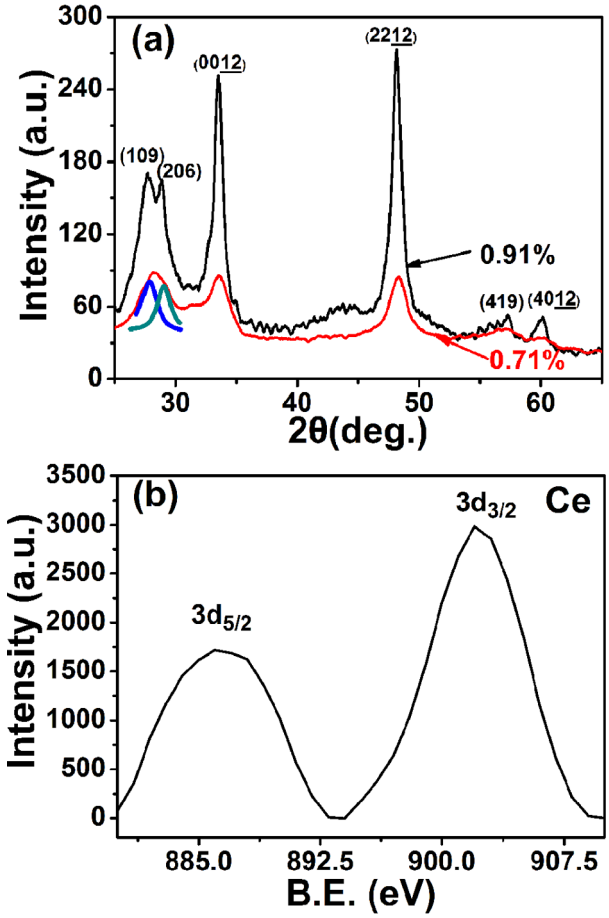

Fig. 2 (a) XRD patterns of In_2S_3:Ce nanoparticles with dopant content 0.71% and 0.91%, and the red broad peak is fitted by the green and pink peaks; (b) Ce 3d X-ray Photoelectron Spectroscopy (XPS) spectrum of the In_2S_3:Ce nanoparticles.

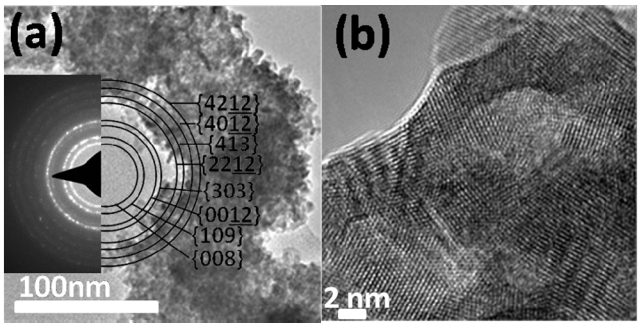

Fig. 3 HRTEM images of In_2S_3:Ce nanoparticles. (a) the morphology and electron diffraction ring; (b) the lattice fringes of particles and the interplanar spacing.

Considering the effect of doped ions , the emission spectra (PL) of In_2S_3 and In_2S_3:Ce nanoparticles in anhydrous alcohol solution using excitation at 370 nm are shown in Fig. 4(a). The PL feature of In_2S_3 nanoparticles exhibits three strong and broad emission bands centered at about 462.5 nm, 432.5 nm and 405.4 nm, repectively. The blue emission is mainly attributed to the

presence of several deep trap states or defects in the structure, and two UV emission bands may also be attributed to quantum-confined effects of In_2S_3 nanoparticles. The three emission bands slightly reveal blue shift compared with the reported data of In_2S_3 nanoparticles (30nm),[21] likely due to increased quantum size confinement of the smaller particles.[22] The emission spectra of In_2S_3:Ce nanoparticles shows shift to the short wavelength, this phenomenon corresponded to the report of the emission spectra of In_2S_3 and $In_{1.8}Eu_{0.2}S_3$,[23] indicating that the quantum efficiency of In_2S_3:Ce is stronger than that of In_2S_3 nanoparticles. In addition, the In_2S_3:Ce nanoparticles shows higher PL intensity than it obtained in In_2S_3 nanoparticles. It is suggested that the doped induces increasing the defects density giving rise to radiative transition and enhances PL intensity.[24] Thus, the doped is conducive to visible light emission activity.[25] In Fig. 4(b) shows the emission spectra of In_2S_3:Ce nanoparticles with dopant content 0.71% and 0.91%. Ce^{3+} ions are good luminescence centers, and the emission band peaks at 523 nm and 520 nm coming from the 5d-4f transitions are detected. The PL intensity increased with increasing Ce content. It confirms the Ce doping and Ce is in the Ce^{3+} state. The effect of doping on optical properties has been widely accepted, meanwhile, it is also an effective means to confirm the doped ions. The dopant adsorbed on the particle surfaces provide surface passivation, so that the exciton does not trap easily to the surface states. Some studies suggest that surface-adsorbed Mn^{2+} on ZnS [26] or CdS [27]

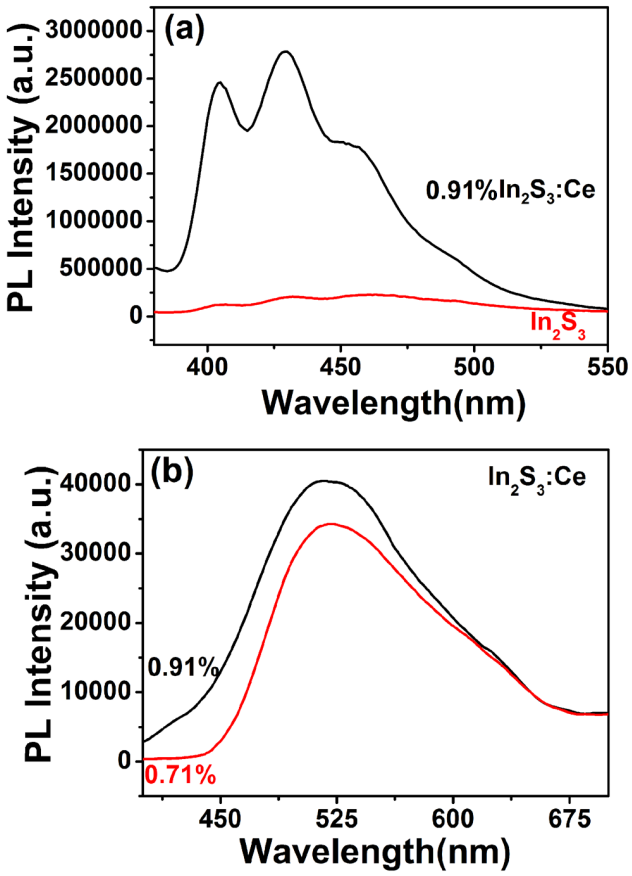

Fig. 4 (a) Photoluminescence spectra (PL) of In_2S_3 and In_2S_3:Ce with dopant content 0.91% nanoparticles in absolute ethyl alcohol solution using excitation at 370 nm; (b) the Photoluminescence spectra (PL) of In_2S_3:Ce with dopant content 0.71% and 0.91%.

nanoparticles is not luminescent, while Mn^{2+} doped into the lattice are responsible for emission. Thus, the PL measurement proves the existence of Ce in the structure.

Fig. 5 shows the study of magnetic property carried out by MPMS SQUID experimental facilities. The Fig. 5(a) displays the variation of magnetization loops for In_2S_3:Ce nanoparticles at 10K, 150K, and 300K in a field between -60 and 60 kOe. The magnetization decreases from 0.024 to 0.008 emu/g at 60 kOe as temperature increases from 10 to 300K. Furthermore, the remanence magnetization and coeretively decrease as temperature increases. The Fig. 5 (b) exhibits the zoom region between -900 and 900 Oe to show more clearly the hysteresis loop. It is seen that the hysteresis loops are irreversible, while the irreversibility of the hysteresis loops are extremely small, suggesting the presence of superparamagnetic behavior which is the characteristic of the ferromagnetic particle with small size.[7] The

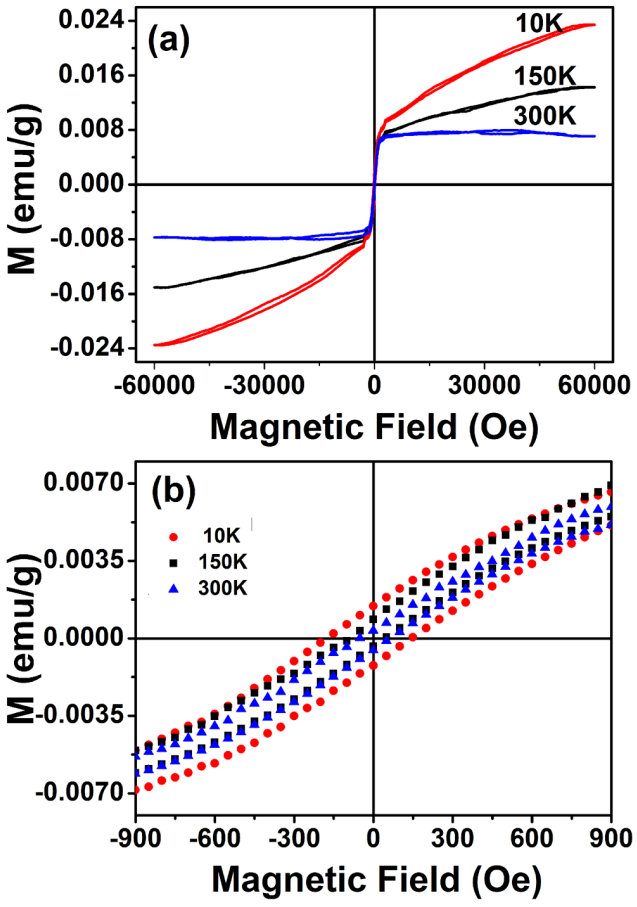

Fig. 5 (a) Magnetization plots of In_2S_3:Ce nanoparticles as a function of the applied fields (-60 and + 60 kOe) at 10 K, 150 K and 300 K; (b) The enlarged view in the field between -900 and 900 Oe at 10 K, 150 K and 300 K.

hysteresis loop areas decrease as temperature increases from 10 to 300 K, indicating a transition of ferromagnetic to superparamagnetic state.[3]

To gain insight into the superparamagnetic property and magnetic transition for In_2S_3:Ce nanoparticles, the temperature dependence of magnetization ZFC-FC curves were measured. Fig. 6 shows the zero-field-cooling (ZFC) and field-cooling (FC) curves of the In_2S_3:Ce nanoparticles with dopant content 0.71%

and 0.91% measured at an applied magnetic field of 500Oe. ZFC magnetization increases as the temperature reduces from 400 K and reaches a maximum at the blocking temperature. The classically thermal-assisted superparamagnetic is blocked at the T_B, forwarding the phase transition from superparamagnetic state to magnetic long-range order.[28] Moreover, the existence of irreversibility between the FC and ZFC branches of the susceptibility below the blocking temperature (T_B) presents the typical behavior of superparamagnetic particles.[4] More interesting, another transition at lower temperature is also observed. ZFC magnetization reaches a minimum near temperature T_C, and starts increasing from this point to T_B. This remarkable transition point gives a clear-cut evidence of Quantum tunneling of magnetization (QTMs) from magnetic long-range order to QSP state in the In_2S_3:Ce nanoparticles with dopant content 0.71% and 0.91% at T_C. This phenomenon is consistent with reports of such behavior at the nanoscale.[7,9,28] Both the ZFC and FC branches decrease with the decrease of temperature, which can be ascribed to the existence of the antiferromagnetic-coupled. In addition, the blocking temperature (T_B=340K) and magnetization of In_2S_3:Ce with Ce content 0.91% is larger than that of In_2S_3:Ce (T_B=300K) with Ce content 0.71%. It is suggested that the larger Ce ions doping causes the higher blocking temperature (T_B) and larger magnetization.

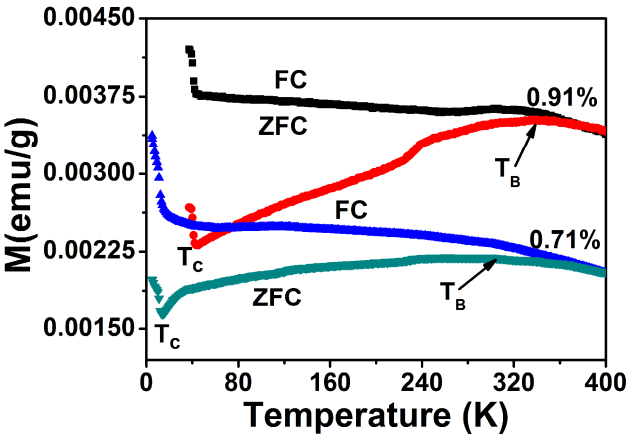

Fig. 6 Magnetization versus temperature for field cooled (FC) and zero-field-cooled (ZFC) measurements, the blocking temperature (T_B) and the critical phase transition temperature (T_C) are indicated on the ZFC data set.

In conclusion, the origin and phase transition of magnetism are closely related to the Ce ions in In_2S_3:Ce nanoparticles. Because of the special electronic structure of rare earth elements, the 4f electrons in Ce are tightly bound around the nucleus and shielded by $5s^2p^6d^16s^2$ electrons, leading to the strong local spin. It is difficult for In_2S_3:Ce nanoparticles to have the 4f-4f exchange interaction without mediums. According to the Ruderman-Kittle-Kasuya-Yoshida (RKKY) model,[29] the localized f electrons make the nomadic s electrons spin polarization as mediums, leading to the 4f-4f exchange interaction, that is the cruise electrons transfer exchange interaction in two local spins without interaction. The origin of magnetism is the Ce doping. The distribution of Ce ions influences the characteristics of magnetic interaction. The Ce-Ce distances in these Cerich zones are short and they favor antiferromagnetic interactions; the Ce-Ce right distances is to promote ferromagnetic interactions; some other Ce atoms may be almost isolated exhibiting paramagnetic behavior.[30] The complicated magnetic behavior of In_2S_3:Ce nanoparticles as the reduction of temperature suggests there are two magnetic transition: the classical thermally driven from SP to blocked SP and the quantum phase transition from magnetic long-range order to QSP state. The doping ion radius size plays an important role on the magnetic phase transition of In_2S_3:Ce nanoparticles.[31] The larger ratio of doped cation to cation radius of structure causes the more defects, leading to the larger concentration of electrons and holes.[32] The size of doping ion radius influences the bond angle, thereby changing the matrix element which describes electron hopping and electronic charge concentration, resuling in changing the temperature of magnetic phase transition.[12] The Ce radius (1.034Å) is larger than In radius (0.8Å), increasing the bond angle and the matrix element which describes electron hopping, leading to the larger carrier concentration in the In_2S_3:Ce nanoparticles. The larger Ce ions doping causes the higher blocking temperature (T_B), showing ferromagnetic at room temperature (340K). The superparamagnetism appears when the thermal energy can overcome the magnetic energy barrier as the decrease of size. And the thermal fluctuation is frozen as temperature decreases, causing a long-range magnetic order. The quantum phase transition from magnetic long-range order to QSP state appears when the size further reduces to small enough. The In_2S_3:Ce nanoparticles are 5-6nm. Dramatic increase in surface to volume ratio causes strong surface anisotropic field to frustrate and disorder the surface spin, which provides channels for quantum tunneling.[33] The SP state can be re-observed due to the Magnetic quantum tunneling even when the thermal energy is smaller than the barrier height. Thus, one can observe the secondary magnetic phase transition from magnetic long-range order to QSP state.

Conclusions

In summary, the high purity Ce-doped In_2S_3 samples without any impurity or secondary phases have been synthesized by a facile gas-liquid phase chemical deposition, as demonstrated by XRD, XPS, and HRTEM. And the PL exhibits that the Ce^{3+} ions doped have enhanced photoluminescence intensity and visible light emission activity, and provide reliable evidence about the existence of Ce into the In_2S_3 nanoparticles. The study of magnetic property testifies that the classical thermally driven from SP to blocked SP and the quantum phase transition from magnetic long-range order to QSP state exist in In_2S_3:Ce nanoparticles. The introduction of Ce causes the larger carrier concentration, increasing the blocking temperature and showing ferromagnetic at room temperature.

Acknowledgements

This work was funded by the National Science Foundation of China, Nos. 11174103, 90923032 and 20873052.

Notes and references

[a] *State Key Laboratory of Superhard Materials, Jilin University, Changchun, 130012, People's Republic of China.*
[*] *Corresponding authors:*
Prof. Mingzhe Zhang，E-mail:zhangmz@jlu.edu.cn
[b] *Institute of physics and telecommunications engineering, Shaanxi University of Technology, Hanzhong, 723000, People's Republic of China.*

1 S. Sapra, D. D. Sarma, S. Sanvito and N. A. Hill, *Nano Lett.*,

2002, **2**, 605.
2 K. Jayanti, S. Chawla, H. Chander and D. Haranath, Cryst. Res. Technol., 2007, 42, 976.
3 C. C. Huang, T. Y. Liu, C. H. Su, Y. W. Lo, J. H. Chen and C. S. Yeh, *Chem. Mater*., 2008, **20**, 3840.
4 O. D. Jayakumar, H. G. Salunke, R. M. Kadam, Manoj Mohapatra, G. Yaswant and S. K. Kulshreshtha, *Nanotechnology*, 2006, **17**, 1278.
5 J. Tejada, R. F. Ziolo and X. X. Zhang, *Chem. Mater*., 1996, **8**, 1784.
6 D. J. Norris, N. Yao, F. T. Charnock and T. A. Kennedy, *Nano Lett*., 2001, **1**, 3.
7 B. B. Yao, R. Zhao, S. Y. Lu, P. Wang and M. Z. Zhang, *RSC Adv*., 2013, **3**, 13878.
8 D. A. Schwaartz, K. R. Kittilstved and D. R. Gamelin, *Appl. Phys. Lett*., 2004, **85**, 1395.
9 W. W. Zheng, P. Kumar, A. Washington, Z. X. Wang, N. S. Dalal, G. F. Strouse and K. Singh, *J. Am. Chem. Soc.*, 2012, **134**, 2172.
10 T. T. Hu, M. Z. Zhang, S. D. Wang and Q. J. Shi, *Cryst. Eng. Comm.*, 2011, **13**, 5646.
11 B. Martínez, F. Sandiumenge, Ll. Balcells, J. Arbiol, F. Sibieude and C. Monty, *Phy. Rev. B*, 2005, **72**, 165202.
12 H. Y. Hwang, S-W. Cheong, P. G. Radaelli, M. Marezio and B. Batlogg, *Phys. Revi. Lett*., 1995, **75**, 914.
13 D. K. Nagesha, X. R. Liang, A. A. Mamedov, G. Gainer, M. A. Eastman, M. Giersig, J. J. Song, T. Ni, and N. A. Kotov, *J. Phys. Chem. B*, 2001, **105**, 7490.
14 X. B. Cao, L. Gu, L. J. Zhuge, W. H. Qian, C. Zhao, X. M. Lan, W. J. Sheng, and D. Yao, *Colloids and surfaces A: Physicochem. Eng. Aspects*, 2007, **297**, 183.
15 J. J. Ning, K. K. Men, G. J. Xiao, L. Y. Zhao, L. Wang, B. B. Liu and B. Zou, *J. Coll. Inter. Sci.*, 2010, **347**, 172.
16 G. X. Cao, Y. B. Zhao and Z. S. Wu, *J. Alloy. Comp*., 2009, **472**, 325.
17 A. Datta, S. Gorai and S. Chaudhuri, *J. Nanopart. Res*., 2006, **8**, 919.
18 W. Chen, J. O. Bovin, A. G. Joly, S. P. Wang, F. H. Su and G. H. Li, *J. Phys. Chem. B*, 2004, **108**, 11927.
19 D. R. Mullins, S. H. Overbury and D. R. Huntley, *Surf. Sci*., 1998, **409**, 307.
20 M. Veith, S. Mathur, A. Kareiva, M. Jilavi, M. Zimmer and V. Huch, *J. Mater. Chem*., 1999, **9**, 3069.
21 (a) G. X. Cao, Y. B. Zhao and Z. S. Wu, *J. Alloy. Compd*., 2009, **472**, 325; (b) B. O. Dabbousi, J. Rodriguez-Viejo, F. V. Mikulec, J. R. Heine, H. Mattoussi, R. Ober, K. F. Jensen and M. G. Bawendi, *J. Phys. Chem. B*, 1997, **101**, 9463.
22 (a) C. Petit, A. Taleb and M. P. Pileni, *Adv. Mater.*, 1998, **10**, 259; (b) F. D. Angelis and L. Armelao, *Phys. Chem. Chem. Phys.*, 2011, **13**, 467.
23 R. S. Mane and C.D. Lokhande, *Mater. Chem. Phys.*, 2002, **78**, 15.
24 H. Li, H. Q. Bao, B. Song, W. J. Wang and X. L. Chen, *Solid State Comm.*, 2008, **148**, 406.
25 H. G. Sun, W. L. Fan, Y. L. Li, X. F. Cheng, P. Li, J. C. Hao and X. Zhao, *Phys. Chem. Chem. Phys.*,2011, **13**, 1379.
26 K. Sooklal, B. S. Cullum, S. M. Angel and C. J. Murphy, *J. Phys. Chem.*, 1996, **100**, 4551.
27 G. Counio, S. Esnouf, T. Gacoin and J.-P. Biolot, *J. Phys. Chem.*, 1996, **100**, 20021.
28 C. Xiao, J. J. Zhang, J. Xu, W. Tong, B. X. Cao, K. Li, B. C. Pan, H. B. Su and Y. Xie, *Scientific Reports*, 2012, **2**, 755.
29 Y. Utsumi, J. Martinek, H. Imamura, P. Bruno and S. Maekawa, *J. Magn. Magn. Mater.,* 2007, **310**, 1142.
30 W. B. Mi, X. C.Wang and H. L. Bai, *Appl. Surf. Sci.*, 2011, **257**, 5698.
31 P. Shiffer, A. P. Ramirez, W. Bao and S. W. Cheong, *Phys. Rev. Lett.*, 1995, **75**, 3336.
32 (a) Y. Mori, N. Niiya, T. Mizuno, T. Nishii, A. Fujii, Y. Fujii, K. Takarabe, Y. Wang and J. Z. Jiang, *Phys. Stat. Sol.*, 2007, **244**, 234 ; (b) Y. Wang, Y. Zhang, W. J. Chang, G. L. Lu, J. Z. Jiang, Y. C. Li, J. Liu and T. D. Hu, *J. Phys. Chem. Solids.*, 2005, **66**, 1775 ; (c) Y. S. Xu, H. Y. Zhu, C. L. Ma, P. W. Zhu, R. D. Cong, X. X. Wu, W. Gao and Q. L. Cui, *J. Solid State Chem*., 2013, **202**, 33.
33 C. T. Hsieh and J. T. Lue, *Physics Letters A*, 2002, **300**, 636.